Materials and Design 81 (2015) 59–64

Contents lists available at ScienceDirect

Materials and Design

journal homepage: www.elsevier.com/locate/matdes

# Formation of highly thermal stable $Al_{88}Ni_6Y_6$ amorphous composite by graphene addition design

Zhenxi Sun [a], Qi Xing [a], Eugen Axinte [b], Wenjuan Ge [a], Jinfeng Leng [a], Yan Wang [a,*]

[a] School of Materials Science and Engineering, University of Jinan, 336 Nan Xinzhuang West Road, Jinan 250022, PR China
[b] Gh. Asachi Technical University of Iasi, Faculty of Machine Manufacturing & Industrial Management, 59 A, Prof. Dimitrie Mangeron Blvd., Romania

ARTICLE INFO

*Article history:*
Received 14 January 2015
Revised 27 April 2015
Accepted 9 May 2015
Available online 11 May 2015

*Keywords:*
Graphene
Thermal stability
Mechanical alloying
Amorphous composite
Al-based alloy

ABSTRACT

We study the effect of graphene (Gr) addition on the amorphisation and thermal stability of the $Al_{88}Ni_6Y_6 + x$ wt.% Gr ($x = 0$, 0.2, 0.5, and 0.8) alloys during mechanical alloying. The final milling-products consist of the amorphous phase and a few nanocrystals with face-centered cubic (fcc) structure, and the AlNiY(Gr) amorphous composites have been fabricated. We find that the 0.2 wt.% Gr addition obviously benefits the amorphisation and remarkably enhance the onset crystallization temperature of the alloy. Continuous heating transformation diagram shows that the as-milled Gr additional alloys need longer time than the $Al_{88}Ni_6Y_6$ alloys to begin to transform into crystals, indicating the Gr addition design enhances the thermal stability of the as-milled $Al_{88}Ni_6Y_6$ alloy. The influence mechanism of Gr addition has been discussed based upon the negative heat of mixing, atomic-size mismatch, diffusion-asymmetry, and special structure of Gr.



## 1. Introduction

Al-based amorphous alloys as environmental friendly materials have attracted more and more attention because of their potential applications in aerospace and transportation field, due to their low density, high specific strength and corrosion-resistant property in recent years [1–3]. The predominant Al-based amorphous alloys include Al-transition metal (TM)–rare earth metal (RE), such as Al–Ni–Y/Gd/La [4–6], Al–Ni–Y–Co–La [7], and Al–Fe–Ce [8] systems. However, the widespread usages of these Al-based amorphous alloys in practical engineering fields are severely hindered by small size material restricted by low glass-forming ability (GFA) and thermal stability [3]. The microalloying technique has been used to effectively improve the GFA and thermal stability, and change the crystallization process of Al-based amorphous alloys [9–11]. The B addition could increase the activation energy for crystallization of the $Al_{87}Y_8Ni_5$ amorphous alloy from 159 up to 228 kJ/mol [9]. The thermal stability of the Al–Ni–La amorphous alloys has been enhanced with increasing the La contents, and the crystallization mode has also been changed from two-stage to three-stage one [11]. Although, some efforts have been made to enhance the GFA and thermal stability of Al-based amorphous alloys, the improvement is insignificant. Mechanical alloying (MA) is regarded as an effective process paralleling to the rapid solidification technique with specific advantages [12]. For the MA method, the high cooling rate is not necessary, and the alloy composition can be more flexible [13]. So far, quite a few Al-based amorphous powders have been prepared by the MA technique [14–18].

Graphene (Gr), a perfect two-dimensional (2-D) lattice of $sp^2$-bonded carbon atoms [19,20], has recently attracted tremendous attention due to its excellent properties, such as excellent thermal conductivity (5000 W $m^{-1}$ $K^{-1}$), high Young's modulus (1 TPa) and fracture strength (125 GPa) [21,22]. Recently, A few studies about influence of Gr addition on the characteristics of metal alloys have been reported [23–25]. The addition of 0.18 wt.% Gr to Mg–1 wt.% Al–1 wt.% Sn alloy leads to an increase in tensile strength (i.e., from 236 to 269 MPa) [23]. Shin et al. [24] selected multi-walled carbon nanotube (MWCNT) and few-layer Gr as a reinforcing agent and prepared aluminum matrix composites, showing that the yield stress for Gr was 3.5 times higher than that of MWCNT. Yan et al. [25] have reported that the Gr reinforced aluminum alloy nanocomposite showed good mechanical properties.

However, little attention has been paid to the addition of Gr to improve the GFA and thermal stability of Al-based amorphous alloy. Thus, it is interesting to investigate how Gr affects the thermal stability and GFA of Al-based amorphous alloy. In this study, the $Al_{88}Ni_6Y_6$ alloys and the Gr are selected as the matrix and additional material, respectively. Using the MA method, we have explored the effects of Gr addition on the amorphisation and thermal stability of the $Al_{88}Ni_6Y_6$ composites, and attempted to discuss

* Corresponding author.
*E-mail address:* mse_wangy@ujn.edu.cn (Y. Wang).

http://dx.doi.org/10.1016/j.matdes.2015.05.028
0261-3069/

the mechanism of minor addition. The consolidation process needs to be optimized for obtaining amorphous–nanophase composites with a desirable structure and high thermal stability. In the present study, the AlNiYGr amorphous composites with the high thermal stability are very conducive to be consolidated into Al-based bulk metallic glass (BMG) composite.

## 2. Experimental

Powder mixtures of elemental Al, Ni, Y, and Gr with nominal compositions of $Al_{88}Ni_6Y_6$ + $x$ wt.% Gr ($x$ = 0, 0.2, 0.5, and 0.8) were mechanically alloyed in a high-energy ball mill (Fritsch P6) at a rotation speed of 300 rpm (revolutions per minute). The chromium steel vial and balls were used in the present work. MA was carried out at room temperature in an Ar atmosphere with a ball-to-powder weight ratio of 15:1. In order to avoid an increase in the vial temperature, the milling procedure was periodically interrupted every 0.5 h and then halted for 0.5 h. In addition, the milling process was interrupted at various time intervals in order to remove small amounts of the milled products for analysis and characterization. Moreover, it needs to note that Gr used in the present study has an Brunauer–Emmett–Teller (BET) surface area of 700 $m^2/g$ and a purity of >99 wt.%, which was prepared by the thermal expansion reduction of Gr oxides. The SEM image of Gr is shown in Fig. 1, which presents the few-layer Gr nanosheets.

The phase constitution of the as-milled powders was identified by X-ray diffraction (XRD, Rigaku D8 Advance) in the Bragg–Brentano geometry using Cu Ka radiation ($\lambda$ = 0.15406 nm). Microstructural characterizations of the as-milled powders were performed on a field emission scanning electron microscopy (FESEM), transmission electron microscopy (TEM) coupled with selected area electron diffraction (SAED). The thermodynamic temperatures of the as-milled powders were investigated by the differential scanning calorimetry (DSC, Mettler-Toledo) at a heating rate of 20 K $min^{-1}$ under a continuous flow of purified argon.

## 3. Results and discussions

Fig. 2 shows the XRD patterns of the as-milled $Al_{88}Ni_6Y_6$ powders with different Gr additions after the selected MA times. At the early stage of ball milling (40 h), the as-milled $Al_{88}Ni_6Y_6$ is a polycrystalline mixture, as indicated by the sharp Bragg-peaks corresponding to Al, Ni, $Y_2O_3$, and $Al_{1.1}Ni_{0.9}$ phases, as shown in Fig. 2(a). With increasing the milling time up to 80 h, the Ni and $Y_2O_3$ phases disappear. The as-milled powders are composed of Al and $Al_{1.1}Ni_{0.9}$ phases, and the corresponding diffraction peaks become obviously broadening, indicating that the grain size gradually decreases, and the lattice strain increases. After 140 h of MA, the diffraction pattern of $Al_{88}Ni_6Y_6$ shows a broadly amorphous background, compared with the baseline (marked as the dash line). However, two crystalline peaks from the reflections of (111), (200), (220) and (311) planes superimpose onto the broad diffuse halo, indicating the formation of the face-centered cubic (fcc) phases. Prolonging the milling time up to 200 h, a very broad diffuse halo coexisting with few fcc-phases exists at $20° < 2\theta < 50°$, implying the formation of the Al-based amorphous composite. Fig. 2(b) presents that the microstructure evolution for the as-milled $Al_{88}Ni_6Y_6$ + 0.2 Gr wt.% powders is similar to the as-milled $Al_{88}Ni_6Y_6$ alloys free of Gr from the milling time 40–140 h. After the milling time of 200 h, the amorphous phase is dominant in the as-milled powders together with only one fcc-peak at about 45°. In order to explore the mechanical stability of the amorphous phase against MA, the powders with 0.2 Gr wt.% addition were continuously milled from 240 to 280 h under the same ball-milling condition. It presents that one weak crystal peak still exists, and the milling products of $Al_{88}Ni_6Y_6$ + 0.2 Gr wt.% consist of amorphous matrix and a few nanocrystals. The $Al_{1.1}Ni_{0.9}$ phases for the $Al_{88}Ni_6Y_6$ + 0.5 Gr wt.% sample are not found after the milling time of 40 h, compared to the 0.2 wt.% and free of Gr additions (Fig. 2(c)). It suggests that the 0.5 wt.% Gr addition can restrain the alloying reaction between the Al and Ni elements at the initial milling time. However, a small amount of $Al_{1.1}Ni_{0.9}$ phases are formed after the MA time from 80 to 140 h. With the increase of the MA time to 200 h, it shows the presence of a broad diffuse hump with two fcc-peaks at about the 38° and 45°. Prolonging the milling time from 240 to 280 h, one crystal peak at the lower angle (38°) disappears. The milling product of the 0.5 Gr wt.% addition is still the amorphous composite with a small amount of nanocrystals. The XRD patterns of the as-milled $Al_{88}Ni_6Y_6$ + 0.8 wt.% Gr powders presented in Fig. 2(d) are also similar to those for the 0.5 wt.% Gr addition (Fig. 2(c)) before the milling time of 40 h. Prolonging the milling time from 80 to 140 h, the diffraction peak of Ni phase at about 76° disappears. After 200 h of the MA, $Al_{1.1}Ni_{0.9}$ phases are formed, indicating that the more additional contents of Gr can further delay the formation of the $Al_{1.1}Ni_{0.9}$. In addition, a small amount of amorphous phases appear together with Al phases. With increasing the milling time to 240 h, the amorphous background compared with the baseline becomes broader and four fcc-peaks still exist. After the milling time of 280 h, two crystal peaks at the higher angle disappear. The amorphous composite with a few nanocrystals is obtained by the 0.8 wt.% Gr addition. In order to qualitatively identify the degree of amorphisation for the test alloys, the proportion of the amorphous phase ($v_A$) of the as-milled $Al_{88}Ni_6Y_6$ + $x$ wt.% Gr ($x$ = 0, 0.2, 0.5, and 0.8) powders after 200 h of the MA time was calculated and are 82.5%, 85%, 80.7% and 52.8%, respectively. It is obvious that the 0.2 wt.% Gr addition can acquire the largest $v_A$ value of 85%, remarkably enhancing the amorphisation.

To verify the XRD results, the as-milled $Al_{88}Ni_6Y_6$ + 0.8 wt.% Gr alloy at 280 h of milling time was selected to be examined using TEM and the corresponding SAED pattern, as shown in Fig. 3. The as-milled particles present different sizes in the range of 0.2–1 μm (Fig. 3(a)). It is also observed that the small particles aggregate together and the particles have some distinct edges and corners (Fig. 3(b)), indicating that the repeated cold-welding and fracture happen during the ball-milling process. The corresponding SAED pattern (Fig. 3(c)) is a diffuse halo, indicating the amorphous nature of the particle. Fig. 3(d) presents another corresponding SAED pattern, which consists of diffraction rings, indicative of the nanocrystalline characteristic of the associated microstructure. The different rings are indexed as (111), (200), and (220)

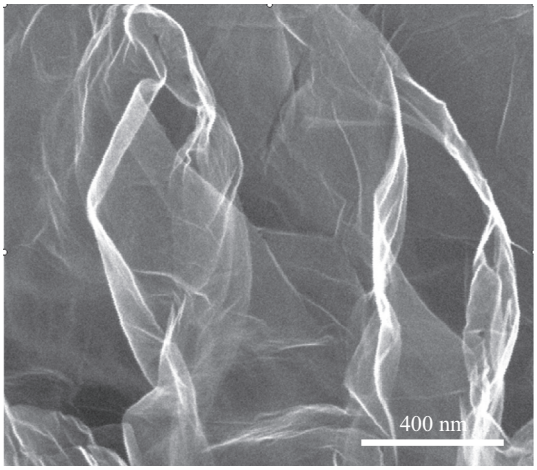


**Fig. 1.** SEM image of additional Gr used in the present study.